Adaptive Shock Testing and Failure Prediction of Printed Circuit Boards Using Kriging-Based Experimental Design

Trotter Roberts[1], Matthew Burnett[1], Ryan Yount[1], Austin R.J. Downey[1,2,*], Adriane Moura[3], and Fahad Abumohaimed[4]

[1]Department of Mechanical Engineering, University of South Carolina, Columbia, SC 29208
[2]Department of Civil and Environmental Engineering, University of South Carolina, Columbia, SC 29208
[3]Applied Research Associates Inc, Niceville, FL 32578
[4]Air Force Research Laboratory, Munitions Directorate, Eglin AFB, FL 32542

ABSTRACT

Printed Circuit Boards (PCBs) are essential components in almost all electronic systems, yet their mechanical durability under shock loading remains difficult to predict due to the complexity of dynamic interactions during impact. In particular, understanding how a combination of different loading conditions, such as acceleration magnitude and impulse duration, affect failure mechanisms is critical for ensuring product reliability across industries. In this study, a data-driven approach is presented to create a surrogate model of PCB failure under drop-test conditions. A comprehensive dataset is generated through repeated drop testing of PCBs, comprising over fourteen individual tests spanning acceleration levels from approximately 5000 to 12000 g and pulse durations ranging from 0.130 to 0.330 ms. For each test, the number of drops to failure is recorded, with observed lifetimes varying from single-impact failure to more than sixty-five drops. This effort seeks not only to catalog performance under impact but also to extract a functional relationship that enables prediction across a continuous space of input conditions. To maximize the information gained from a limited number of experiments, we employ a Kriging-based iterative design approach, termed KRISP-U, that adaptively identifies regions of high model uncertainty. Using an initial subset of the experimental data as seed points, a surrogate model is constructed to estimate failure response across the test space. A cross-validation approach using Kullback-Leibler divergence is then used to quantify surrogate model uncertainty and inform the selection of subsequent test conditions. This iterative process yields an increasingly accurate model while minimizing the total number of physical tests required. The result is a robust failure prediction map, capable of estimating PCB survivability over the investigated range of shock magnitudes and pulse durations. This map not only accelerates durability assessments for new designs but also establishes a foundation for a broader class of predictive tools that relate dynamic loading conditions to structural failure. The presented methodology highlights the value of adaptive experimental design in mechanical reliability testing and underscores its scalability for future studies in electronics durability and structural health monitoring.

Keywords: failure prediction, shock testing, printed circuit boards, kriging, uncertainty quantification, surrogate modeling.

1. INTRODUCTION

Printed circuit boards serve as the structural and electrical backbone of nearly all modern electronic systems, and their failure under shock and impact loading can compromise entire assemblies, leading to costly repairs or catastrophic system downtime in applications such as aerospace, automotive safety systems, and defense electronics.[1] While standardized drop and impact tests are widely used to evaluate PCB durability,[2,3] predicting survivability across a broad range of shock conditions, particularly for high-rate and high-amplitude events

*Contact author: Austin Downey; Email: austindowney@sc.edu

occurring over microsecond-to-millisecond time scales, remains a fundamental challenge.[4] The dynamic response of PCBs to impact is highly nonlinear and influenced by acceleration magnitude, pulse duration, boundary constraints, and internal mass distribution, resulting in complex and often unpredictable failure modes.[5,6]

Traditional durability assessments typically rely on fixed test matrices in which selected acceleration levels or pulse shapes are evaluated in isolation.[7,8] Although these tests provide baseline survivability metrics, they fail to capture the continuous relationship between shock parameters and failure probability.[9] Exhaustive physical testing across the full range of potential loading conditions is impractical due to time, cost, and sample size constraints, particularly in high-rate environments where loading uncertainty and short event durations limit experimental throughput. Consequently, qualification decisions often rely on interpolation between sparse test points, leaving significant gaps in understanding how combined loading conditions govern the onset of mechanical and electrical failure in PCBs.

Surrogate modeling approaches provide an effective means of addressing these limitations by approximating complex input–output relationships using limited experimental data.[10] Gaussian process regression, also known as kriging, is well-suited for reliability and fatigue studies because it provides both a predictive response surface and a quantitative measure of uncertainty.[11] When paired with adaptive experimental design,[12,13] kriging enables experiments to be focused on the most informative regions of the input space, reducing experimental burden while improving model fidelity. This study introduces a data-driven, kriging-based framework for predicting PCB failure under drop-test conditions, in which peak acceleration magnitude, pulse duration, and the number of drops to failure are used to iteratively construct a failure prediction map. Kullback–Leibler divergence is employed as an information metric to guide test selection and systematically reduce predictive uncertainty.

The primary contributions of this work are threefold. First, it introduces an adaptive experimental design framework for PCB drop testing that maximizes the informational value of limited test data. Second, it develops a surrogate modeling approach that captures the joint influence of acceleration magnitude and pulse duration on PCB failure behavior. Finally, it demonstrates how uncertainty quantification can be used to guide test selection and accelerate the development of predictive failure maps for electronics durability and structural health monitoring.

2. METHODOLOGY

A combined experimental and modeling framework was employed to characterize PCB failure behavior under mechanical shock, thereby minimizing the total number of tests. Drop experiments were conducted over a range of acceleration magnitudes and pulse durations to obtain failure data. These results were used to construct a Kriging-based surrogate model of the failure response, which provides both predictions and associated uncertainty. An iterative refinement process was then applied, in which uncertainty estimates guided the selection of additional test conditions, allowing for the efficient development of a predictive failure map.

2.1 Experimental Design

Printed circuit boards fabricated from 175 Tg FR4 were used as test specimens. Each board had effective dimensions of 25.40 mm × 88.9 mm × 1.60 mm and contained a single 1 kΩ, 2 W surface-mount resistor soldered at midspan using a controlled stencil-based process to reduce solder joint variability and intentionally limit solder volume so that failure would consistently occur in the resistor solder joints. The boards were mounted as fixed–fixed beams in a custom aluminum fixture, providing rigid boundary conditions and repeatable bending behavior during shock loading. The experimental setup and test-to-failure protocol build upon a previously established shock testing framework for fixed–fixed PCB assemblies.[14] Mechanical shock was applied using a guided drop tower, shown in Fig. 1, with shock severity controlled by adjusting drop height and impact compliance to vary peak acceleration magnitude and pulse duration. The overall test configuration, including sensor placement and data acquisition, is shown schematically in Fig. 2. The data associated with this publication is available through a public repository.[15]

Acceleration input was measured using an Endevco 7280A-60k piezoresistive accelerometer mounted on the shock table, while PCB response was measured using an Endevco 72-20K accelerometer mounted near the component location. Acceleration signals were sampled at 2 MHz, and peak acceleration and effective pulse duration were extracted from the measured time histories for each drop event. At each acceleration–pulse duration condition, repeated drop events were applied to a specimen until failure occurred, defined as an open-circuit condition in the surface-mount resistor. The number of drops to failure was recorded for each test condition.

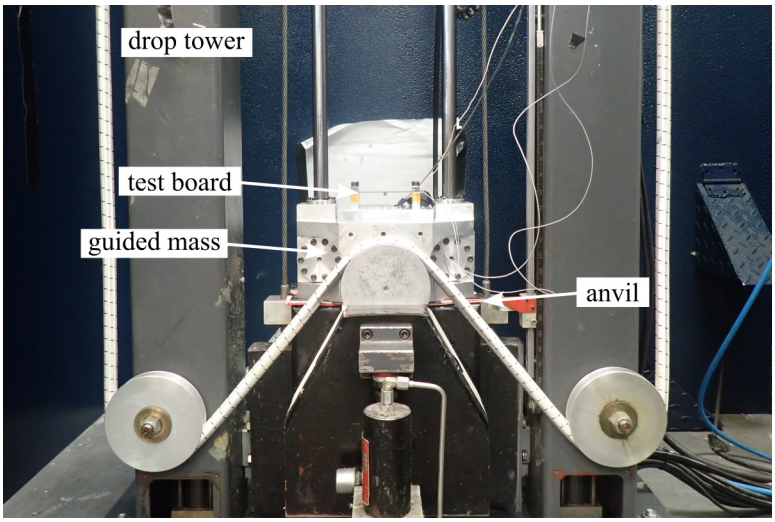

Figure 1: Drop tower used for mechanical shock testing.

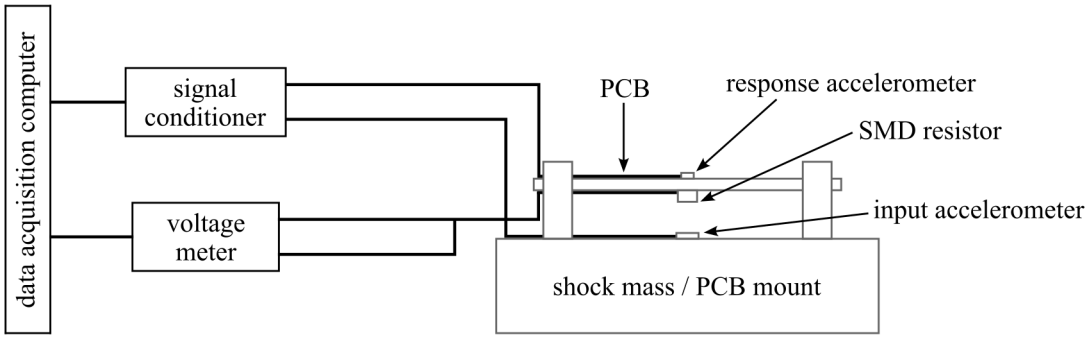

Figure 2: Diagram of the experimental setup and instrumentation.

2.2 Surrogate Modeling

To enable prediction of PCB survivability across a continuous range of shock conditions, a kriging-based surrogate model was constructed to map shock input parameters to the measured impacts-to-failure response. Each experiment provides an input vector

$$\mathbf{x} = \begin{bmatrix} a \\ \tau \end{bmatrix}, \tag{1}$$

where a is the measured peak acceleration magnitude and τ is the effective pulse duration extracted from the table acceleration time history (Fig. 4). The experimental response is the observed number of drops to failure associated with each input condition.

A universal kriging (UK) surrogate was selected because it captures both global trends and local spatial variability in the response while remaining data-efficient for sparse experimental campaigns. In UK, the predicted failure response field is decomposed into a deterministic drift (trend) component and a spatially correlated stochastic residual,

$$y(\mathbf{x}) = m(\mathbf{x}) + \varepsilon(\mathbf{x}), \tag{2}$$

where $m(\mathbf{x})$ is a low-order regression model and $\varepsilon(\mathbf{x})$ is modeled as a second-order stationary random field with covariance defined through a variogram model. A Gaussian variogram was selected to represent a smooth response surface over the acceleration–duration domain.

For a given dataset $\mathcal{D}_N = \{(\mathbf{x}_i)\}_{i=1}^{N}$, the fitted UK model was evaluated over a fixed Cartesian grid spanning the current experimental domain,

$$a \in [a_{\min}, a_{\max}], \qquad \tau \in [\tau_{\min}, \tau_{\max}]. \tag{3}$$

This produces a gridded prediction field $P(\mathbf{x})$ that estimates impacts to failure throughout the domain. The prediction field serves as the continuous failure surface used in subsequent analysis, while the common gridded representation enables direct field-to-field comparisons required by the KRISP-U uncertainty procedure described next.

2.3 Adaptive Test Point Selection (KRISP-U)

Additional experiments were selected using a KRISP-Uncertainty strategy (KRISP-U) that quantifies model sensitivity spatially using leave-one-out cross-validation (LOOCV) and Kullback–Leibler divergence (KLD).[16,17] The procedure follows the workflow shown in Fig. 3 and identifies regions of the (a, τ) domain where the surrogate prediction remains under-informed.

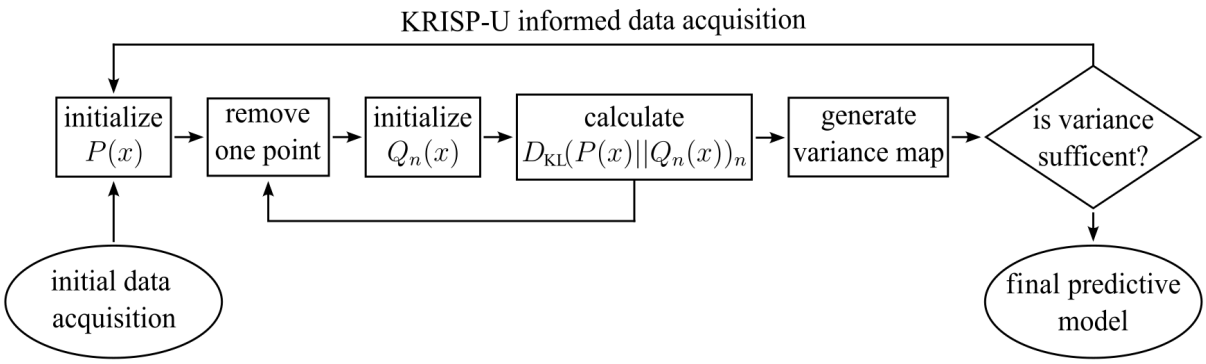

Figure 3: KRISP-U workflow used for uncertainty-informed test selection.

At each iteration, a full-data UK model is trained on D_N and evaluated on the common grid to produce a reference prediction field, denoted $P(\mathbf{x})$ in Fig. 3. One non-boundary observation is then removed and a new surrogate is trained on the reduced dataset to generate a leave-one-out prediction field $Q_n(\mathbf{x})$, where the subscript n denotes the omitted point. This remove–refit procedure is repeated for each removable observation.

The influence of point n on the predicted failure surface is quantified by computing the KLD between the full-data prediction field and the corresponding leave-one-out field, yielding a scalar variance (uncertainty) score assigned to that point,

$$v_n = D_{\mathrm{KL}}(P(\mathbf{x}) \parallel Q_n(\mathbf{x}))\,. \tag{4}$$

In practice, $P(\mathbf{x})$ and $Q_n(\mathbf{x})$ are evaluated on the common grid and vectorized prior to computing the divergence metric, such that v_n reflects the change in the entire predicted failure surface induced by removing point n. Larger values of v_n indicate regions where the surrogate prediction is highly dependent on a single observation and therefore remains poorly constrained.[17]

To maintain stability of the sampled domain boundary, the first N_b observations (designated boundary points) are never removed during LOOCV; their variance scores are set to zero. After computing discrete scores $\{(\mathbf{x}_n, v_n)\}_{n=1}^{N}$, a continuous variance map $v(\mathbf{x})$ is constructed via scattered interpolation of the point scores over the grid,

$$v(\mathbf{x}) = \text{Interp}\left(\{\mathbf{x}_n, v_n\}\right), \tag{5}$$

and normalized by its maximum value for consistent visualization across iterations. The next test condition is then selected from this variance map, most simply as

$$\mathbf{x}_{N+1} = \arg\max_{\mathbf{x}\in\mathcal{X}} v(\mathbf{x}), \tag{6}$$

where $\mathcal{X}$ denotes the feasible test space. To reduce sensitivity to isolated local maxima, an alternative selection rule may be used in which the weighted centroid of the largest connected region above a chosen variance threshold is selected. In all cases, the selected condition is executed experimentally, appended to the dataset, and the cycle in Fig. 3 is repeated until the variance map is deemed sufficient for prediction.

2.4 Validation and Performance Metrics

Model convergence and predictive improvement were evaluated using field-level discrepancy metrics computed on the common prediction grid. After completion of the experimental campaign, a UK model trained on the full dataset was used to generate a reference prediction field, denoted $P_{\text{ref}}(\mathbf{x})$. For an intermediate surrogate trained on the first k data points, the corresponding prediction field is denoted $P_k(\mathbf{x})$. The global discrepancy between fields was quantified using the Kullback–Leibler divergence,

$$D_{\text{KL},k} = D_{\text{KL}}(P_{\text{ref}}(\mathbf{x}) \parallel P_k(\mathbf{x}))\,, \tag{7}$$

which provides a scalar measure of how closely the intermediate surrogate approximates the final predictive failure surface.

Because extrapolation outside the experimentally sampled region can dominate error metrics without being physically meaningful, performance metrics were evaluated only within the convex hull of the sampled points. A hull-based mask was applied to prediction and error fields prior to computing summary statistics, ensuring that reported improvements reflect interpolation behavior within the supported experimental domain.

In addition, a standard error metric was computed on the grid to provide a physically interpretable measure of prediction accuracy,

$$\text{RMSE}_k = \sqrt{\frac{1}{N_g}\sum_{j=1}^{N_g}(P_{\text{ref},j} - P_{k,j})^2}, \tag{8}$$

where N_g is the number of grid points and index j enumerates the flattened prediction grid.

3. RESULTS AND ANALYSIS

The experimental campaign and adaptive modeling process produced a progressively refined dataset that revealed the relationship between drop-test parameters and PCB survivability. Initial test results establish baseline trends in failure behavior, while successive iterations of the Kriging model reduce uncertainty and improve predictive accuracy. The final surrogate model yields a continuous failure prediction map, validated against withheld data and interpreted to identify reliability trends. Together, these results demonstrate the effectiveness of uncertainty-driven experimental design for accelerating durability assessments in electronic systems.

Table 1: Summary of drop-test data sets.

data set	mean pulse width (ms)	mean peak acceleration (kg_n)	ΔV (km/s)	impacts to failure	class
1	0.175	5.387	5.888	65	boundary
2	0.099	12.211	7.550	2	boundary
3	0.329	5.401	13.222	19	boundary
4	0.218	10.446	14.222	1	boundary
5	0.132	7.691	6.340	2	boundary
6	0.145	10.254	9.286	4	operator
7	0.187	9.788	11.431	1	operator
8	0.205	9.364	11.988	1	operator
9	0.252	8.162	12.845	3	operator
10	0.164	10.260	10.508	1	algorithmic
11	0.185	8.858	10.234	3	algorithmic
12	0.207	6.111	7.900	13	operator
13	0.319	6.469	12.888	3	operator
14	0.212	6.045	8.004	6	algorithmic

3.1 Experimental Data

Fourteen drop-test data sets were collected across a range of peak acceleration magnitudes and pulse durations to populate the failure response space for the PCB assemblies. The dataset includes boundary-defining tests selected to establish the limits of the experimental domain, interior test points chosen by engineering judgment, and algorithmically selected conditions identified using the KRISP-U adaptive sampling strategy.

Table 1 summarizes the experimental conditions, observed impacts to failure, and classification of each test. The boundary tests span both high-survivability regimes, where failure occurs after many impacts at lower acceleration magnitudes, and rapid-failure regimes characterized by single- or few-impact failure at high acceleration. Interior and operator-selected points populate the central portion of the design space, capturing variability introduced by pulse duration at comparable acceleration levels. Algorithmically selected points target regions identified by the KRISP-U framework as under-resolved, improving coverage of the failure response surface.

Representative acceleration time histories from selected drop tests are shown in Fig. 4. These traces illustrate the shock profiles applied during testing and the extraction of the two key input parameters used in surrogate modeling: peak acceleration magnitude and effective pulse duration.

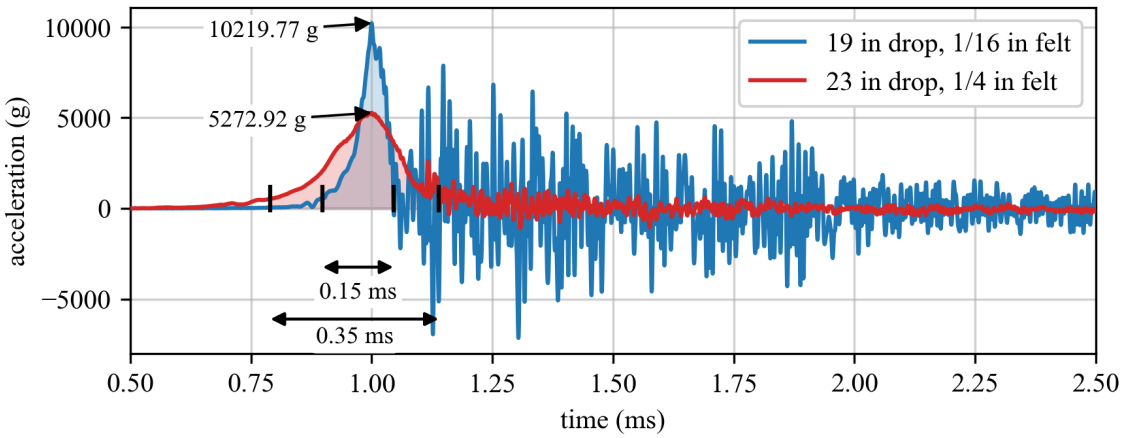

Figure 4: Representative acceleration time histories showing extraction of peak acceleration and effective pulse duration.

Although the acceleration pulses exhibit similar overall shapes, Fig. 4 highlights measurable variation in both peak magnitude and pulse width arising from changes in drop height and impact compliance. These variations contribute directly to differences in the observed impacts-to-failure response. Consistent with expectations for shock-driven solder joint failure, higher peak acceleration magnitudes generally correspond to failure after fewer impacts. However, Table 1 also shows that pulse duration introduces additional variability in survivability, particularly at intermediate acceleration levels where similar peak accelerations produce markedly different impact counts. This coupled dependence on acceleration magnitude and pulse duration motivates the two-parameter surrogate modeling approach and the adaptive experimental design strategy employed in this study.

3.2 Model Development

The surrogate model was developed iteratively as experimental data were added using the KRISP-U adaptive sampling framework. Beginning with a small seed dataset composed of boundary-defining experiments and limited interior points, a universal kriging surrogate was trained to estimate impacts to failure across the acceleration–pulse duration domain. This initial model provides a coarse approximation of the failure surface and serves as the baseline for subsequent refinement.

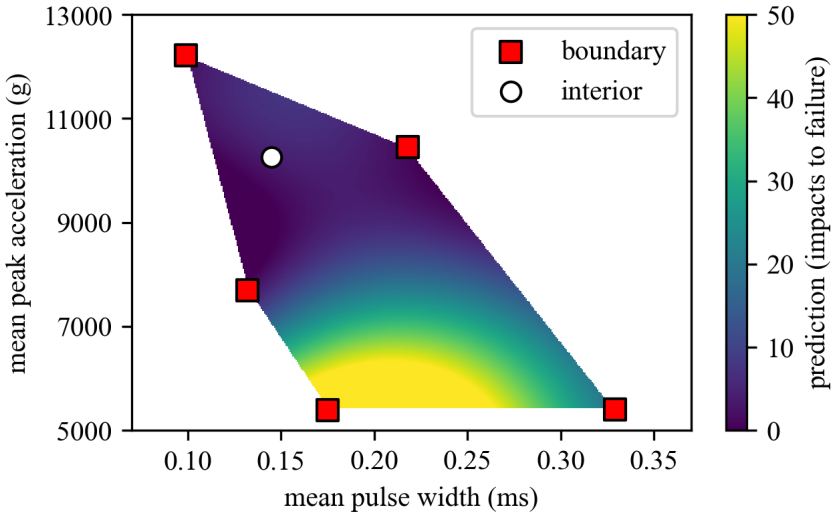

Figure 5: Initial kriging-based failure prediction surface constructed from the seed dataset.

Figure 5 shows the initial kriging-based failure prediction surface constructed from the seed dataset. At this stage, the surrogate captures broad trends in failure behavior but remains weakly constrained across much of the design space due to limited data coverage.

As additional experiments were conducted, the surrogate model and its associated uncertainty were updated following each iteration of the KRISP-U workflow. The evolution of the surrogate prediction surface and corresponding KRISP-U uncertainty map is shown in Fig. 6. Panels (a)–(d) correspond to surrogate models constructed after 1, 3, 5, and 9 added interior data points, respectively.

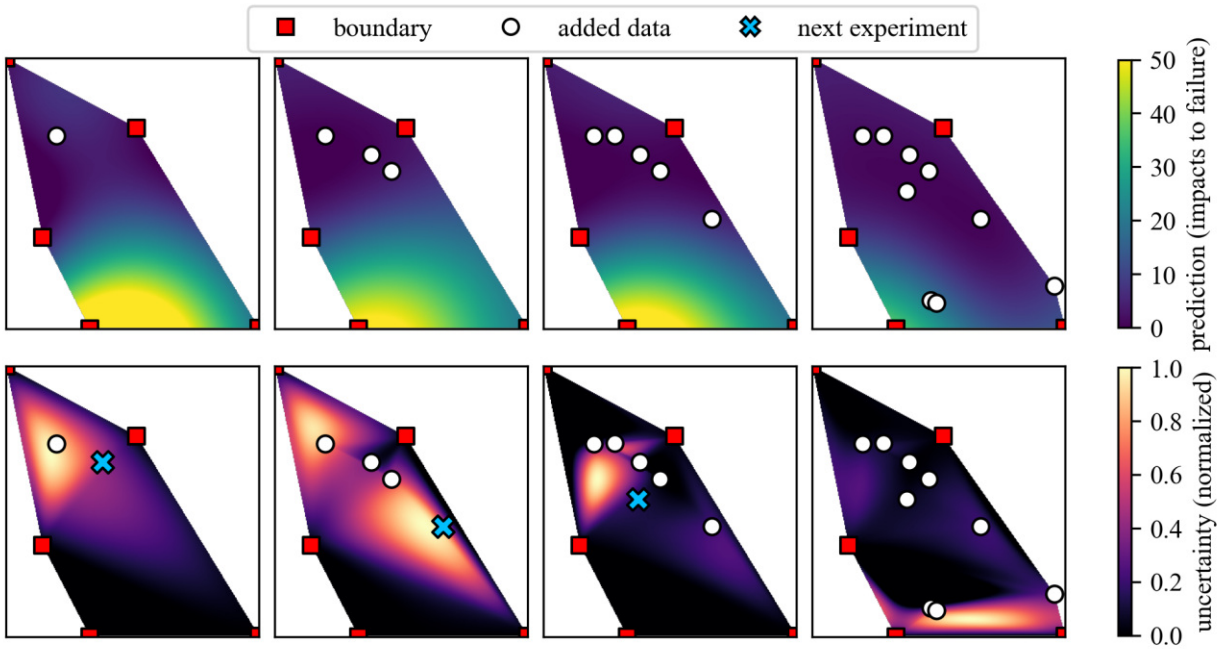

Figure 6: Evolution of the surrogate prediction surface and corresponding KRISP-U uncertainty map for (a) 1, (b) 3, (c) 5, and (d) 9 added interior data points.

With each iteration, regions of high uncertainty become more localized and move toward sparsely sampled regions.KRISP-U consistently identifies areas where the predicted surface is most sensitive, which guides subsequent test selection. While experimental variability and practical constraints prevent exact execution at the algorithmically optimal location, the selected test conditions closely follow the dominant uncertainty regions.

The final failure prediction surface obtained after completion of the adaptive testing campaign is shown in Fig. 7. This final surrogate model predicts PCB failure with low and well-quantified uncertainty.

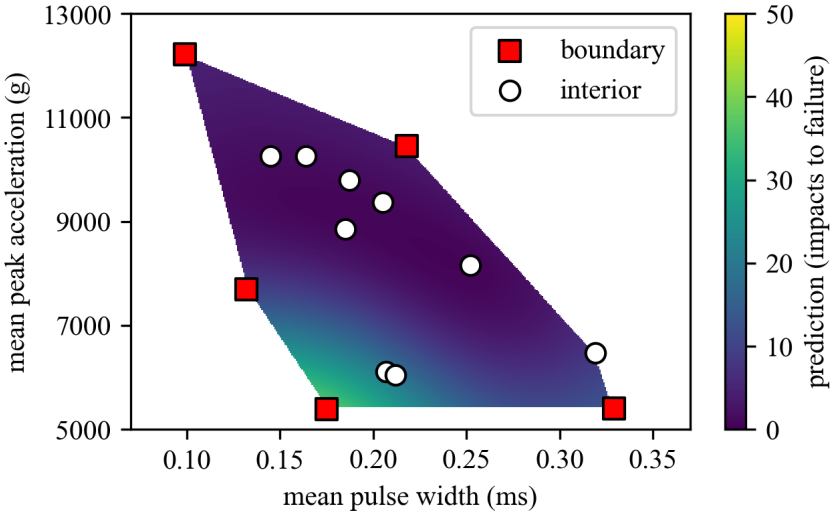

Figure 7: Final converged kriging-based failure prediction map after completion of the adaptive testing campaign.

3.3 Evaluation and Discussion

The effectiveness of the KRISP-U adaptive sampling strategy was evaluated by tracking changes in surrogate model uncertainty and prediction error as additional experimental data was incorporated. Field-level discrepancy metrics were computed on a common prediction grid, enabling direct comparison between intermediate surrogate models and the final converged model.

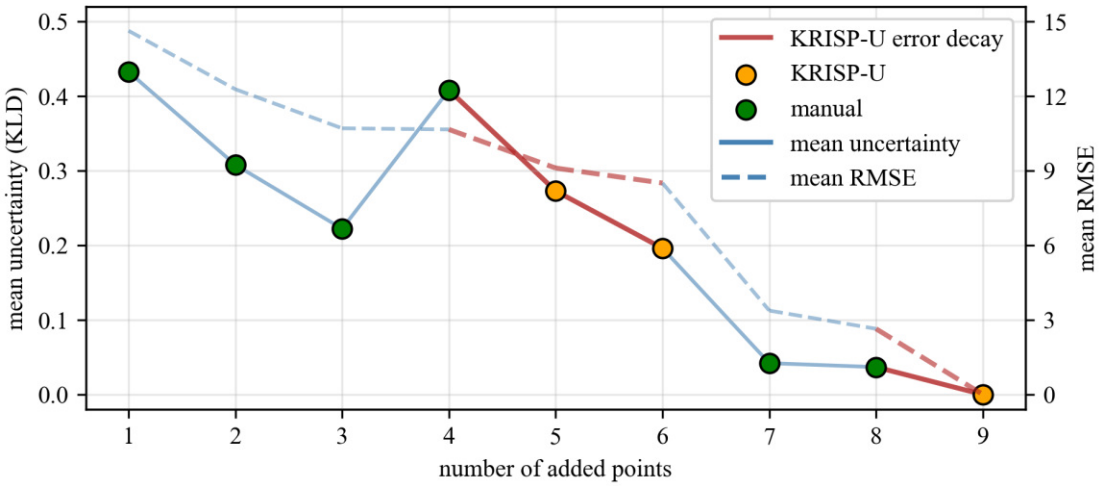

Figure 8: Surrogate model mean uncertainty and RMSE as additional experimental data are incorporated into the model.

Figure 8 shows the evolution of the mean KRISP-U uncertainty metric as additional drop-test data points are incorporated into the model. Decreases in mean Kullback–Leibler divergence indicate improved agreement between intermediate surrogate predictions and the final reference field, while concurrent reductions in error demonstrate improved numerical accuracy of the failure surface. Iterations in which new experiments were selected using the KRISP-U strategy exhibit more consistent reductions in uncertainty compared to manually selected points, validating the effectiveness of uncertainty-informed sampling for accelerating surrogate model convergence.

The failure prediction map developed in this study enables continuous assessment of PCB shock survivability across coupled acceleration and pulse-duration conditions, extending beyond traditional discrete qualification tests. By identifying regions of rapid change in survivability, the model highlights operating regimes where design margins are limited and where targeted design modifications may be most effective.

For qualification testing, the KRISP-U adaptive framework provides a data-efficient means of characterizing failure behavior by prioritizing experiments in regions of high uncertainty. This approach reduces the total number of physical tests required while maintaining predictive confidence, which is particularly beneficial for high-rate shock environments. Although demonstrated for a single PCB configuration, the methodology is readily extendable to other board designs, assemblies, and reliability metrics, providing a scalable framework for adaptive electronics durability assessment.

4. CONCLUSION

Predicting printed circuit board (PCB) survivability under mechanical shock remains challenging due to the coupled influence of acceleration magnitude, pulse duration, and test-to-test variability. Traditional qualification approaches based on fixed test matrices provide limited insight into this multidimensional failure space and require extensive experimental effort. This study addressed these limitations by developing an adaptive, data-driven framework for PCB drop-test failure prediction.

An uncertainty-informed surrogate modeling approach was introduced using universal kriging in combination with the KRISP-U adaptive experimental design strategy. Starting from a limited seed dataset, the methodology iteratively refined a continuous failure prediction surface relating acceleration magnitude and pulse duration to impacts to failure. By quantifying model sensitivity using leave-one-out cross-validation and Kullback–Leibler divergence, new experiments were systematically selected in regions where they provided the greatest information gain. The resulting surrogate model converged rapidly, yielding a robust failure prediction map while minimizing the number of required physical tests.

The results demonstrate that uncertainty-driven test selection can significantly improve modeling efficiency and predictive confidence for PCB shock reliability assessments. Beyond the specific PCB configuration studied here, the proposed framework is readily extensible to other board geometries, component layouts, and dynamic loading scenarios. Future work will focus on incorporating additional design and environmental variables, integrating electrical degradation metrics, and coupling data-driven surrogates with physics-based models to further enhance predictive capability for electronics subjected to high-rate mechanical loading.

5. ACKNOWLEDGMENTS

This material is based upon work supported by the National Science Foundation grant numbers CCF - 1956071, CCF-2234921, and CPS - 2237696. Additional support was provided from the Air Force Office of Scientific Research (AFOSR) through award number FA9550-21-1-0083. and from the Air Force Research Laboratory (AFRL) under HII Prime Contract No. FA8075-18-D-0002, Task Order No. FA8075-24-F-0022, through Subcontract No. P000073237 to the University of South Carolina. Any opinions, findings conclusions, or recommendations expressed in this material are those of the authors and do not necessarily reflect the views of the National Science Foundation or the United States Air Force. The experimental data and associated analyses used in this work are approved for public release under Distribution Statement A (Approved for public release; distribution unlimited), AFRL-2026-0036.

REFERENCES

1. Esser, B., Huston, D. R., and Miller, J., "Aerospace electronics weight reduction through the use of active mass damping," in [*Smart Structures and Materials 2003: Damping and Isolation*], Agnes, G. S. and Wang, K.-W., eds., **5052**, 433–444, SPIE (July 2003).
2. "JESD22-B104C: Mechanical shock," (Nov. 2004). Test method standard.
3. Luan, J.-e., Tee, T. Y., Pek, E., Lim, C. T., and Zhong, Z., "Dynamic responses and solder joint reliability under board level drop test," *Microelectronics Reliability* **47**, 450–460 (Feb. 2007).
4. Dodson, J., Downey, A., and Laflamme, S., "High-rate structural health monitoring: Part-I introduction & data," in [*IMAC XLI Proceedings*], (feb 2023).
5. Dodson, J., Downey, A., Laflamme, S., Todd, M. D., Moura, A. G., Wang, Y., Mao, Z., Avitabile, P., and Blasch, E., "High-rate structural health monitoring and prognostics: An overview," in [*Data Science in Engineering, Volume 9*], 213–217, Springer International Publishing (2021).
6. Zhu, L. and Marcinkiewicz, W., "Drop impact reliability analysis of csp packages at board and product levels through modeling approaches," *IEEE Transactions on Components and Packaging Technologies* **28**, 449–456 (Sept. 2005).
7. Wong, E., Mai, Y., Seah, S., Rajoo, R., Lim, T., Lim, C., and Field, J., "Drop impact reliability - a comprehensive summary," in [*2005 Conference on High Density Microsystem Design and Packaging and Component Failure Analysis*], 1–11, IEEE (June 2005).
8. "JESD22-B111: Board level drop test method of components for handheld electronic products," (July 2003). Test method standard.
9. Steinberg, D. S., ed., [*Vibration analysis for electronic equipment*], John Wiley & Sons, New York, 3rd ed. (2000).
10. Forrester, A. I. J., Sóbester, A., and Keane, A. J., [*Engineering Design via Surrogate Modelling: A Practical Guide*], Wiley (July 2008).

11. Rasmussen, C. E. and Williams, C. K. I., [*Gaussian processes for machine learning*], Adaptive computation and machine learning, MIT Press, Cambridge, Mass. [u.a.], 3rd ed. (2008).
12. Jones, D. R., Schonlau, M., and Welch, W. J., "Efficient global optimization of expensive black-box functions," *Journal of Global Optimization* **13**, 455–492 (Dec. 1998).
13. Echard, B., Gayton, N., and Lemaire, M., "AK-MCS: An active learning reliability method combining kriging and monte carlo simulation," *Structural Safety* **33**, 145–154 (Mar. 2011).
14. Roberts, T., Luck, H., Satme, J. N., Gol Zardian, M., Navidi, S., Yount, R., Downey, A. R. J., and Hu, C., "Test-to-failure characterization and acceleration signal feature analysis of electronic systems under repeated shock loading," in [*IMAC XLIV Proceedings*], (jan 2026). In Proceedings of IMAC-XLIV.
15. Yount, R., Burnett, M., Roberts, Trotter, Downey, A. R., Moura, A., and Abumohaimed., F., "Dataset 14 PCB shock testing acceleration and pulse duration." https://github.com/High-Rate-SHM-Working-Group/Dataset-14-PCB-Shock-Testing-Acceleration-and-Pulse-Duration (2026).
16. Kullback, S. and Leibler, R. A., "On information and sufficiency," *The Annals of Mathematical Statistics* **22**(1), 79–86 (1951).
17. Burnett, M., Zhang, T., Downey, A. R. J., and Lang, Y., "Surface roughness surrogate modeling in metal 3D printing using kriging and batch experimental design," in [*Volume 2A: 45th Computers and Information in Engineering Conference (CIE)*], *IDETC-CIE2025*, American Society of Mechanical Engineers (Aug. 2025).